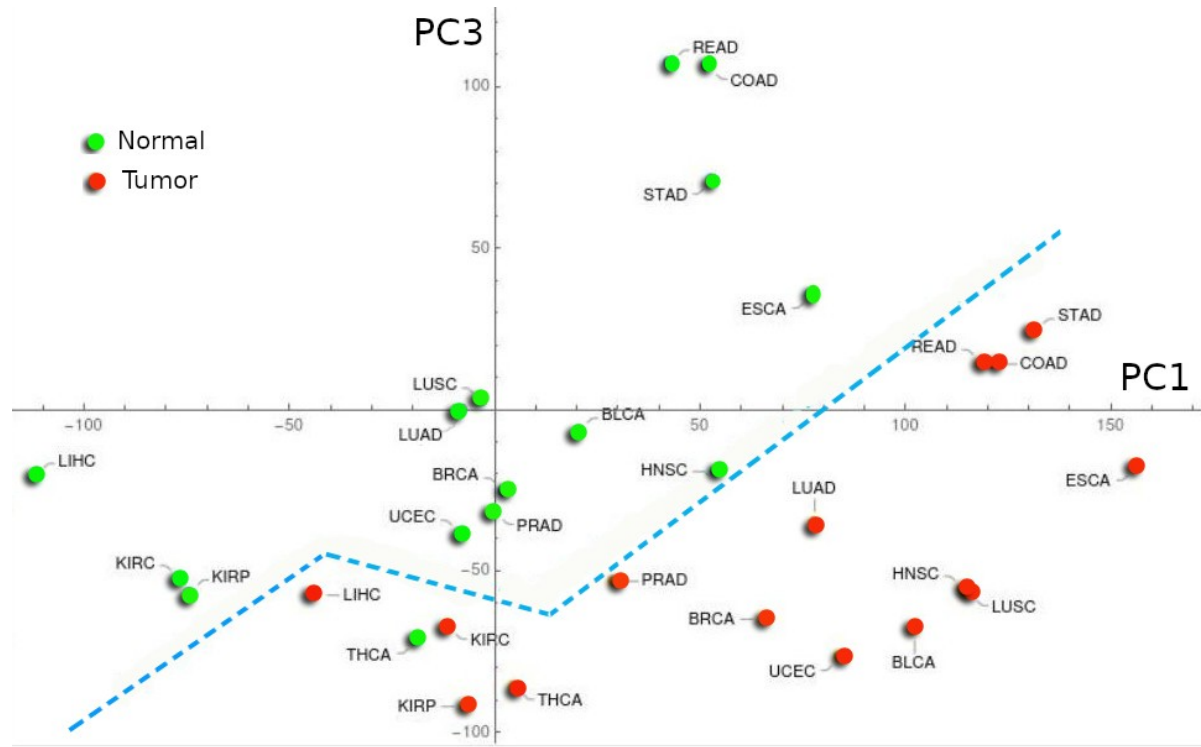


On the gene expression landscape of cancer

Augusto Gonzalez, Yasser Perera, Rolando Perez

GRAPHICAL ABSTRACT



HIGHLIGHTS

The effective dimensionality of the region spanned by normal tissues and tumors in the gene expression space is around 10.

For a given localization, tumors are well separated from normal samples. The tumor region is a kind of attractor.

By analyzing TCGA data for 15 localizations, we can draw a landscape of cancer in the gene expression space, and an approximate border separating normal tissues from tumors.

The distance between tumor centers of a pair of localizations seems to be inversely correlated to the number of shared genes, characterizing the tumor states.

The most dysregulated top pathway in tumors, with regard to the fraction of modified genes participating in it, is related to the "Extracellular matrix organization".

On the gene expression landscape of cancer

Augusto Gonzalez (1,2), Yasser Perera (3,4), Rolando Perez (1,5)

- (1) Joint China-Cuba neuroinformatics laboratory and Academic Unit,
University of Electronic Science and Technology of China, Chengdu, People Republic of China,
augusto@neuroinformatics-collaboratory.org
- (2) Instituto de Cibernetica, Matematica y Fisica, La Habana, Cuba
- (3) China-Cuba Biotechnology Joint Innovation Center, Yongzhou,
People Republic of China
- (4) Centro de Ingenieria Genetica y Biotecnologia, La Habana, Cuba
- (5) Centro de Inmunologia Molecular, La Habana, Cuba

SUMMARY

A principal component analysis of the TCGA data for 15 cancer localizations leads to the following results: The effective dimensionality of the region spanned by normal tissues and tumors in the gene expression state space is around 10 (out of a huge initial space with more than 60000 genes). Gene expression profiles uniquely distinguish between normal and cancer states. For any given tissue, the cancer state is a kind of attractor in the gene expression state space with at least 2500 highly differentially-expressed genes and a power-like tail in the expression distribution function. With regard to this 4% quantile of genes, pairs of localizations share between 314 and 1889 genes characterizing the tumor state. The gene expression landscape shows distances between pairs of tumor localizations which inversely correlate with the number of shared genes. The most significantly altered top pathway in the cancer state is related to the "Extracellular matrix organization".

INTRODUCTION

Cancer is a very complex phenomenon. From one side, the number of internal variables participating in relevant processes in a tissue is huge. The number of human genes, for example, is around 60000. From the other side, as in any aspect of life, ties with the environment are very strong.

Big efforts aimed at understanding basic aspects of cancer have led to many important results (cite: Previous results). Current views include cell-intrinsic (i.e. genetic & epigenetic) and cell-extrinsic phenomena (i.e. micro-environment), as well as population genetics approaches with random drift and directional selection shaping, what has been coined as somatic evolution (cite: Somatic evolution). There is even a plausible hypothesis that cancer is an atavism, that is a cooperative state of multi-cellular organisms, prior to modern metazoa (cite: Metazoans). In spite of this progress, a simple enough picture, quantifying the evolution of a normal tissue towards cancer is still lacking.

The grail in this area would be to describe the functional state of a tissue in terms of a few effective variables, as schematically represented in Fig. 1. In this oversimplified picture, two variables are enough to describe the state. The starting point in the somatic evolution – represented by the origin, corresponds to a healthy young tissue. As time evolves, the interaction of both internal processes (mutations, epigenetic changes, etc) and external factors, may drive an initial bunch of aberrant founder cells and their derived progeny (i.e. a clone) away from the physiologically regulated state. This evolution is schematically represented by arrows in the figure. Eventually, this new cell mass or neoplasm may leave the shaded area, which is the region of “normal” functioning, and move towards cancer.

(Insert Fig. 1)

Once the neoplasm abandons the normal area, we have at our disposal two contentious paradigms of cancer evolution. In the first one the evolution of an aberrant cell population out of the normal tissue region is driven by directional positive selection (cite: Positive selection), but the cancer region is a diffuse one, not well defined in gene expression space.

In the second one, which is called the attractor paradigm (cite: Attractor paradigm), once the clone abandons the normal behavior, it is driven by internal processes to a pre-definite state: cancer, with a precise location in the expression space. In a very reductionistic view one may think, for example, about normal functioning and cancer as two stable solutions of a global gene regulatory network (cite: GRN). As mentioned, one of these states (the normal one) is represented in Fig. 1 as the origin of coordinates, the shaded area would be the normal state basin of attraction. The second attractor, not depicted in Fig. 1, should be the region of confluence of all trajectories out of the normal area.

In the present paper, we show that gene expression data seem to support the attractor picture of cancer, in the sense that a simple processing of the data for a given tissue makes apparent the normal and cancer regions in the expression space. In addition, we find “metagenes” (cite: Metagenes), that is gene profiles characterizing the cancer state, compare these profiles for different localizations in order to show how close their tumors are, etc. The title of the paper, “cancer gene expression landscape”, indicates the aim at placing all tumors in a single plot and delineating the border between normal tissues and tumors.

A glance at results is offered in Fig. 2, which contains Principal Component (PC) analysis (cite: PCA) of the data provided by The Cancer Genome Atlas (TCGA) project (cite: TCGA) for Squamous Cell Lung Cancer (LUSC). The axes are the first two principal components, which accounts for 71 % of the data variance. Note that the regions corresponding to Normal and Tumor tissues are very well defined in the state space.

(Insert Fig. 2)

This second figure may be understood as a realization of the schematic view given in Fig. 1. Points represent the gene expression state of tissue samples (from different individuals) captured at given instants of their somatic evolution histories. The two variables describing the sample state are the first two principal component coordinates. Note that normal and tumor regions are well defined in the state space, in support of the attractor paradigm.

In the paper, we avoid using models or elaborated theoretical constructions that could hide basic facts. Instead of this, we focus on global results following straightforwardly from the expression data. Molecular biology is a very challenging area in which one shall try to infer the behavior of a system with no less than 60000 variables from observations in a few hundred samples. The general laws and state variables are not completely known or understood. It belongs to the realm of complex systems (cite: Complex Systems).

A detailed description of results is presented in the next section.

RESULTS

Instead of attempting the detailed description of the complex internal processes in a tissue, one may try a statistical approach to the phenomenon, in which a reference behavior is set and variables describing departure from the reference state are introduced. Normal and tumor samples, validated

by pathology analysis, are used to look for correlations, apply clustering algorithms, etc. Many of the results presented in Refs. ([cite: Previous Results](#)) are based on such a strategy.

In our paper, however, the emphasis is not on the statistical analysis. We will take the variables following from the PCA, and will try to get from them as much qualitative and semi-quantitative information as possible.

As mentioned, we take expression data for 15 cancer localizations from the TCGA project. This is a well curated database. Gene expressions are measured by sequencing the mRNA produced in the transcription process (RNA-seq, [cite: RNASeq](#)). The data is in the number of fragments per kilo-base of gene length per mega-base of reads format (FPKM, [cite: FPKM](#)).

Reduced dimensionality of the gene expression state space

The first result to stress is the effective dimensionality of gene expression state space, which is not 60000 but a number around 10.

Indeed, recall the PC analysis in LUSC. We forced the reference for the PC analysis to be at the center of the cloud of normal samples. This is what actually happens in a population, where most individuals are healthy and cancer situations are rare. In the Transparent Methods accompanying file, the PC analysis used methodology is explicitly explained.

We take the mean geometric average over normal samples in order to define the reference expression for each gene, and normalize accordingly to obtain the differential expressions, $\bar{e} = e/e_{\text{ref}}$. Finally, we take the base 2 logarithm, $\hat{e} = \text{Log}_2(\bar{e})$, to define the fold variation. Besides reducing the variance, the logarithm allows treating over- and sub-expression in a symmetrical way. The covariance matrix is defined in terms of \hat{e} .

The eigenvectors of the covariance matrix define the PC axes: PC1, PC2, etc, and projection over them define the new state variables. By definition, PC1 captures the highest fraction of the total variance in the sample set. In LUSC, for example, it accounts for 67 % of the variance. It is worth noting that this first PC variable may discriminate between a normal sample and a tumor, as may be clearly seen in Fig 2. PC1 can thus be labeled as the cancer axis.

The following axis, PC2, captures 4 % of the data variance in LUSC, PC3 accounts for 3 %, etc. In some sense, they realize the grail mentioned in the Introduction because with a few such variables we may describe to a considerable extent the complexity of LUSC.

We performed the PC analysis in 15 cancer localizations of the TCGA database, that is, localizations where there are at least 10 normal samples, and the number of tumor samples is greater than 150. The total fraction of variance captured by the first three PC variables is shown in Table I.

This fraction depends on the sample set, and may vary if we enlarge or reduce the set. Thus, we should take the results as approximate, semi quantitative ones, that shall improve as the sample size is enlarged.

Notice that in spite of the statistical origin of the new variables we may use them to describe the actual state of a given sample. Each unitary vector along any of the PC axes defines an expression profile, with a meaning. The fact that with 10 such variables we may account for 90 % or more of the data dispersion means that the effective dimensionality of the state space is much less than it seems. Genes do not take arbitrary expressions, but act in a concerted way. Groups of genes,

metagenes or sub-networks express themselves as profiles.

PC1 is the cancer axis

Let us call \mathbf{v}_1 the eigenvector along PC1 (boldface denotes vectors). We showed above that the PC1 axis accounts for the largest fraction of variance and may be taken as an indicator of the malignant state. For a given sample with fold expression vector $\hat{\mathbf{e}}$, the projection x_1 over the PC1 axis is precisely defined as: $x_1 = \hat{\mathbf{e}} \cdot \mathbf{v}_1$.

The \mathbf{v}_1 vector may be thought to provide a metagene or gene expression profile of cancer in the tissue, i.e. the set of over- or under-expressed genes (and their relative importance) that define the cancer state.

As an illustration, we show in Fig. 3 the 11 genes with the largest contributions to \mathbf{v}_1 in LUSC. In order to simplify the figure, the amplitudes corresponding to the remaining more than 60000 genes are set to zero. Note the signs, positive and negative indicating over- and under-expression respectively. In principle, these genes can be used as markers of the cancer state.

(Insert Fig. 3)

This analysis is promising and have not been sufficiently exploited so far. Below, we should come back to the vector \mathbf{v}_1 .

The expression distribution function

In this paragraph, we show results for the expression distribution function, that is the number of genes with a given differential expression. We shall stress that most of the genes preserve expression values similar to the normal tissue results, that is $\bar{e} \approx 1$. However, there is a heavy tail with a power-like (Pareto, [cite: Pareto](#)) behavior.

We show in Fig. 4 the integrated distribution function, , i.e. the number of genes with normalized expression above \bar{e} , in the over-expression region for all of the tumors studied in the present paper. This number seems to be proportional to $(\bar{e}_{\max}/\bar{e})^a$, where \bar{e}_{\max} is the maximal value taken by \bar{e} , and a is a coefficient between 1.5 (LUSC) and 3 (BLCA). In Table I we report the values of \bar{e}_{\max} for each tumor.

(Insert Fig. 4)

Notice that there are around 1000 genes with differential expression higher than 2. Common wisdom states that the tumor may arise as a result of a few hits on particular (driver) genes ([cite: Driver genes](#)). What we observe from the figure is that once the cancer state is established there are thousands of genes with significant differential expression.

Similar results (not shown) are obtained for the sub-expression tail. There are around 1000 sub-expressed genes with $|\bar{e}| < 1/2$, and the sub-expression profile in tumor tissues exhibits a Pareto distribution. However, for a particular tumor localization, the distribution is not always symmetric, that is the over- and sub-expression tails could be very different.

For each localization, we select the most significant 2500 genes with the largest contributions to the vector \mathbf{v}_1 along the PC1 direction defining the cancer state. This number, although arbitrary, is dictated by the previous results on the expression distribution function. Let us stress that these are genes with significant differential expressions and great importance in the definition of the cancer

state.

In a first rough approach, we may classify tissues according to the fraction of over-expressed genes in the main set of 2500 genes characterizing the tumor. The results are shown in Fig. 5. There are at least three tumors for which the over expression tail is much heavier (LIHC, STAD and ESCA), and four tumors for which silenced genes are dominant (COAD, READ, BRCA and KIRP). In the rest of localizations, the distribution function is nearly symmetric.

(Insert Fig. 5)

We should stress, however, that as we focus on a smaller set, let us say 30 genes, in all the studied cases, with the exception of LUSC and THCA, the most important contributions to the \mathbf{v}_1 vector come from silenced genes.

Dynamics in the expression space

As mentioned above, the cancer region is well defined in the expression space, thus supporting the attractor paradigm. We may study the progression towards cancer by introducing “time” variables. The first such variable is simply the patient age.

We continue using LUSC as an example. According to age, in LUSC we may define 4 subgroups of samples: Normal Young (NY), Normal Old (NO), Tumor Young (TY) and Tumor Old (TO). These subgroups are in some sense arbitrarily defined. First, the label “normal” refers to a pathologically normal sample from a patient with a tumor. Second, in the example “young” labels samples where age is lower than 62 years. These conditions are dictated by the availability of samples, as in any statistical analysis.

Nevertheless, the results are very interesting. The (over-) expression distribution function is visualized in Fig. 6. We compute (mean geometric) averages over the NY, NO, TY and TO subgroups, and use the NY values as references in order to define normalized (differential) expressions in the remaining subgroups: \bar{e}_{NO} , \bar{e}_{TY} , \bar{e}_{TO} . Genes are sorted with regard to their normalized expression values.

(Insert Fig. 6)

There are important deviations for a number of genes in the NO group with regard to the NY reference. This may be taken as a consequence of aging. In tumors, however, deviations are much larger. There are around 1000 over-expressed genes with $|\bar{e}| > 5$.

Most striking is the similarity between the distribution functions in the TY and TO subgroups. For tumors, the distribution function in the final state is nearly independent of the age when tumor initiates. This is an additional argument in favor of the attractor hypothesis. Similar results (not shown) are obtained for the sub-expression tail.

A slightly different “time” variable is provided by the clinically determined tumor stage. It is a qualification given to the tumor at the moment of diagnosis, but in some sense it quantifies also the somatic evolution once the portion of the tissue acquires the tumor condition. Fig. 7 shows the distribution of tumors by stages in Clear Cell Kidney Carcinoma (KIRC). Normal tissues are represented by blue points, whereas tumors are drawn in red. The four panels refer to the four stages: i, ii, iii and iv. Blue points are in the four panels, but only red points with the corresponding stage are included in each panel.

(Insert Fig. 7)

We use a contour plot and colours to visualize the total density of points in the state space. Two regions of maximal density are apparent, corresponding to normal states and an optimal region for tumors. Intuitively, one expects that tumors move along the transition region from the normal to the tumor region as the stage evolves from i to iv. In the actual measurements, we don't track individual tumors as function of stages, but get pictures of different tumors at different stages. Thus, in the initial stages we should observe a fraction of red points captured in the transition region, whereas in the final stages, most tumors should be concentrated in the optimal region. This is what actually follows from the figure, again supporting the attractor paradigm. We may speculate that the optimal region could be related to a region of maximal fitness for the tumor in the given tissue.

All of these characteristics, that is reduced dimensionality of the state space, around 2000 – 2500 genes with $|\hat{e}| > 2$ or even higher, coincidence between the TY and TO distribution functions (wherever the available data allow us to define such subgroups), and a power-like tail, are common to all of the cancer localizations studied in the present paper.

Groups of tumors and Pan-cancer genes

In this paragraph, we consider the question about the altered genes shared by groups of tumors.

Table II shows the number of shared genes for pairs of localizations. Notice that these numbers vary in the interval between 314 and 1889. We may use a threshold, t , of shared genes to define groups of tumors. By definition, a localization is in a group if it shares no less than t genes with at least one tissue in the cluster.

If the threshold is set to 700 shared genes we get the following two groups of tumors: KIRC-KIRP and PRAD-LUSC-LUAD-UCEC-BLCA-ESCA-BRCA-HNSC-COAD-READ-STAD. The remaining 2 localizations (LIHC and THCA) do not form groups, i.e. do not share more than 700 genes with any other tissue. The number of genes common to all of the tumors in the largest group is 49, a relatively large number. These are pan-cancer genes in the sense that they are relevant in the definition of the cancer state in terms of gene expressions in a group of 11 localizations.

We shall further study the implications of these results on shared genes.

Finally, we shall stress that there are six genes common to all of the localizations. They are MMP11 (+), C7 (-), ANGPTL1 (+), UBE2C (-), IQGAP3 (-) and ADH1B (+). It is noteworthy that these genes are straightforwardly related to cancer hallmarks (cite: Hallmarks): i.e. invasion, suppression of the immune response, angiogenesis, proliferation and changes in metabolism. Their differential expressions are very similar in all of the studied tumors. The signs added in parenthesis mean that the gene is over- or under-expressed in tumors.

Below, we rise the question of whether the number of shared genes is related to the proximity of tumors in the expression space.

The gene expression landscape

We consider the central goal of the paper: i.e. to draw a picture in which both normal tissues and tumors in different localizations are represented. We shall use the e_{normal} and e_{tumor} (mean geometric) averages for each localization in order to define cloud centers. The reference is to be computed by averaging over all normal expression vectors. Then, the \hat{e} magnitudes and the

covariance matrix are obtained, and the latter diagonalized.

The first aspect to be stressed is that the first two PCs accounts only for 37 % of the total data variance. The relative importance of these two variables is not so apparent as in the case of individual tissues. This aspect is due to the big dispersion of the data for normal tissues, related to tissue differentiation, sometimes even larger than separations between a normal tissue and the respective tumor.

As a consequence of the dispersion of normal tissues, we do not have a “cancer axis” or direction, as in individual tissues. In order to draw a frontier between normal and tumor regions, we shall include higher PCs. The next component, PC3 accounts for 12 % of the data variance.

We show in Fig. 8 the (PC1, PC3) plane, which indeed suggests that there is a border. We may baptize this figure as the “approximate normal vs cancer plane”. It is apparent from the figure, that the transition from a normal tissue to the corresponding tumor involves simultaneous displacements along the PC1 and PC3 axes.

(Insert Fig. 8)

The unitary vectors along these axes allow the identification of the most significant genes. For example, the 8 most important genes along PC1 are: PI3 (-), ADH1B (+), MYBL2 (-), UBE2C (-), ALB (+), CEACAM5 (-), CST1 (-) and MMP1 (-). Notice that ADH1B and UBE2C were mentioned above as pan cancer genes for this group of 15 tissues.

On the other hand, the 8 most important genes along PC3 are: SLC26A3 (+), DES (+), LGALS4 (+), PHGR1 (+), GPA33 (+), KRT20 (+), GUCA2A (+) and CEACAM5 (+). Notice that the transition to tumors involve also a displacement along the negative direction of PC3, thus the signs (over- or sub-expression) should be reversed.

A more detailed analysis of the border between normal tissues and tumors is required, In the present paper, we limit ourselves to draw the global picture, and leave this analysis for a future work.

Distances in the gene expression space and number of shared genes

In the present paragraph, we would like to provide an interpretation for distances in the gene expression space: the shorter the distance between tumor centers the larger the number of shared genes which define the cancer state.

In Fig. 9 we test the correlation between the number of shared genes in pairs of tumors, computed above, and the distance between tumor centers. A curve (Number of genes = $369 + 58145/\text{distance}$) is drawn for illustrative purposes only, as a guide to the eye.

(Insert Fig. 9)

Notice that these are full distances, not distances in the (PC1, PC3) plane.

The figure shows that we may indeed interpret distances between tumor centers in the gene expression space in terms of the number of altered genes shared by these localizations. Recall that our definition of altered genes is local. It takes as reference the normal gene expression in the tissue, not the global reference used in Fig. 8 to draw the landscape.

We could also test the correlation between distances and shared genes for normal tissues. The

common reference shall be also used, allowing the definition of gene differential expressions for all normal tissues. We leave this exercise on the number of shared genes in tissue differentiation for a future consideration.

Group of tumors and top pathways

A different way of looking for similarities between tumors, instead of a direct comparison of altered genes, is to consider the pathways in which these genes participate and compare the degree of modification of pathways. To this end, we use the same sets of 2500 genes defining the cancer state in these tissues. We took participation of genes in top pathways from the Reactome database ([cite: Reactome](#)). Notice that there are many genes still not annotated in this database.

In order to measure the extent a pathway is modified we count the number of genes participating in it with the corresponding multiplicities. That is, if a gene is called twice in the pathway, we count it two times. The fraction of modified genes gives us a level of pathway distortion. According to this measure, for example, the most distorted pathway in the studied tumors is related to the "Extracellular matrix organization".

Notice that the idea is to compare tumors, not to perform an enrichment analysis ([cite: Enrichment](#)) of pathways in tumors.

In Supplementary Table I, we give the ratio of modified genes in each pathway for each localization. One shall notice that there are pathways for which the fraction of modified genes take low, intermediate or high values for all of the localizations.

In addition, there are distorted pathways with significant variations along tumors, which allow to classify or group tumors. They are: "Chromatin organization", "DNA Repair", "Reproduction", "Cell Cycle" and "DNA Replication". There is an additional pathway with these characteristics, "Digestion and absorption", but we do not include it in the analysis because the number of genes in this pathway is very low (29).

The patterns are shown in Fig. 10. We get two subgroups of localizations and an independent tumor (PRAD).

([Insert Fig. 10](#))

Notice that there are similarities and differences when clustering with regard to the number of shared genes or to the modifications of the relevant pathways. In Fig. 11 we compare both schemes. We shall further study the implications of these findings.

([Insert Fig. 11](#))

DISCUSSION

We performed PC analysis of gene expression data for 15 tumors. Our results are approximate and semi-quantitative, in the sense that they could be modified if a larger data set become available, but at the same time they are simple, general and unbiased, in the sense that no modeling or elaborated mathematical treatments are used. We try to keep interpretation of results as close as possible to the facts.

Both somatic evolution in a normal tissue, and the transition to a tumor state involves the modification of thousands of genes. However, these genes do not act independently, but in a

concerted way. The true number of degrees of freedom of the biological system consistent of a tissue in gene expression space seems to be around 10.

These variables, although of statistical origin, can be used to describe the state and evolution of the tissue, in particular one of the variables measures the progression from normal to cancer state (the cancer axis) and allows the definition of a profile of genes involved in this progression.

The data seem to support the theory of cancer as an attractor, that is once a portion of the tissue escapes from the normal region it is driven to the cancer basin of attraction.

The gene profile of cancer is the first important conclusion, allowing us to speculate about the reversibility of somatic evolution along the cancer axis. Spontaneously, the evolution is in the direction of the cancer state. However, what would happen if we target a few of the most significant genes in the cancer profile? Mathematically, this is a displacement in the reverse direction, but would it actually mean a reverse staging of the tumor? On the other hand, could this kind of intervention induce a rearrangement of the whole profile? These are interesting questions with possible implications for therapy.

Interesting questions are also raised in relation to the second important conclusion of our paper, related to the overall landscape in gene expression space: not only individual tissues are separated from their respective tumors, but the set of normal tissues are separated from the set of tumors. We shall further study the border between the two regions. In a very rough analysis, we noticed that pan cancer genes (i.e, common to all 15 tumors) are involved in the definition of the border. One may dream about designing therapies, following from these conclusions, against groups of tumors.

Work along some of these directions is in progress.

Limitations of the Study

It would be appropriate in the future to include the remaining localizations of the TCGA database, as well as other data. The dependence of the results on the data size, specially on the number of normal samples which is relatively small, should be clarified. The biological significance of many of the results should be further studied, in particular, the found pan-cancer genes, the border between normal tissues and cancer, etc. In the present paper the goal is to get a global picture for the gene expression landscape of cancer, many of the findings should be further clarified.

METHODS

All methods can be found in the accompanying Transparent Methods supplemental file.

SUPPLEMENTAL INFORMATION

Supplemental Information can be found online at <https://doi.org/...>

ACKNOWLEDGMENTS

A.G. acknowledges the Cuban Program for Basic Sciences and the Office of External Activities of the Abdus Salam Centre for Theoretical Physics for support. The research is carried on under a project of the Platform for Bio-informatics of BioCubaFarma, Cuba. The data for the present analysis come from the TCGA Research Network: <https://www.cancer.gov/tcga>.

AUTHOR CONTRIBUTIONS

Conceptualization & Investigation, all authors; Software and formal analysis, A.G.; Writing –

Original Draft, A.G.; Writing – Review & Editing, all authors.

DECLARATION OF INTERESTS

The authors have no competing interests to declare.

REFERENCES

[Previous results]

The ICGC/TCGA Pan-Cancer Analysis of Whole Genomes Consortium (2020). Pan-cancer analysis of whole genomes. *Nature* 578: 82-93.

Moritz Gerstung, Clemency Jolly, Ignaty Leshchiner, et al (2020). The evolutionary history of 2,658 cancers. *Nature* 578: 122-128.

PCAWG Transcriptome Core Group, Claudia Calabrese, Natalie R. Davidson, et al (2020). Genomic basis for RNA alterations in cancer. *Nature* 578: 129-136.

Matthew A. Reyna, David Haan, Marta Paczkowska, et al (2020). Pathway and network analysis of more than 2500 whole cancer genomes. *Nature Communications* 11: 729.

[Somatic evolution]

P.C. Nowell (1976). The clonal evolution of tumor cell populations. *Science* 194: 23-28.

[Metazoans]

P.C.W. Davies and C. H. Lineweaver (2011). Cancer tumors as Metazoa 1.0: tapping genes of ancient ancestors. *Phys. Biol.* 8(1): 015001.

Tomislav Domazet-Lošo and Diethard Tautz (2010). Phylostratigraphic tracking of cancer genes suggests a link to the emergence of multicellularity in metazoa. *BMC Biology* 8: 66.

Charles H. Lineweaver, Paul C. W. Davies and Mark D. Vincent (2014). Targeting cancer's weaknesses (not its strengths): Therapeutic strategies suggested by the atavistic model. *Bioessays* 36: 827-835.

Luis Cisneros, Kimberly J. Bussey, Adam J. Orr, et al (2017). Ancient genes establish stress-induced mutation as a hallmark of cancer. *PLoS ONE* 12(4): e0176258.

Anna S Trigos, Richard B Pearson, Anthony T Papenfuss, and David L Goode (2019). Somatic mutations in early metazoan genes disrupt regulatory links between unicellular and multicellular genes in cancer. *ELife* 8: e40947.

[Positive selection]

P. Vineis and M. Berwick (2006). The population dynamics of cancer: a Darwinian perspective. *Int. J. Epidemiol.* 35: 1151-1159.

R.A. Gatenby (2006). Commentary: Carcinogenesis as Darwinian evolution? Do the math! *Int. J. Epidemiol.* 35: 1165-1167.

[Attractor paradigm]

S.A. Kauffman (1969). Metabolic stability and epigenesis in randomly constructed genetic nets. *Journal of Theoretical Biology* 22(3): 437-467.

S. Huang, G. Eichler, Y. Bar-Yam and D.E. Ingber (2005). Cell fates as high-dimensional attractor states of a complex gene regulatory network. *Phys Rev Lett.* 94(12):128701.

Sui Huang, Ingemar Ernberg, and Stuart Kauffman (2009). Cancer attractors: A systems view of tumors from a gene network dynamics and developmental perspective. *Semin. Cell. Dev. Biol.* 20(7): 869–876.

[Gene regulatory networks]

Eric Davidson and Michael Levine (2005). Gene regulatory networks. *PNAS* 102 (14): 4935.

[Metagenes]

Erich Huang, Skye H Cheng, Holly Dressman, et al (2003). Gene expression predictors of breast cancer outcomes. *The Lancet* 361(9369): 1590-1596.

[PCA]

Svante Wold, Kim Esbensen, and Paul Geladi (1987). Principal component analysis. *Chemometrics and intelligent laboratory systems* 2(1-3): 37-52.

[TCGA]

The TCGA Research Network: <https://www.cancer.gov/tcga>.

[Complex systems]

Hiroaki Kitano (2002). Computational systems biology. *Nature* 420:206-210.

[RNA-seq]

Zhong Wang, Mark Gerstein, and Michael Snyder (2009). RNA-Seq: a revolutionary tool for transcriptomics. *Nat. Rev. Genet.* 10(1): 57–63.

[FPKM]

C. Trapnell et al. (2010). Transcript assembly and quantification by RNA-Seq reveals un-annotated transcripts and isoform switching during cell differentiation. *Nature Biotechnology* 28: 511-515.

[Pareto]

M.E.J. Newman (2005). Power laws, Pareto distributions and Zipf's law. *Contemporary Physics* 46: 323-351.

[Driver genes]

Matthew H. Bailey, Collin Tokheim, Eduard Porta-Pardo, et al (2018). Comprehensive Characterization of Cancer Driver Genes and Mutations. *Cell* 173: 371–385.

[Hallmarks]

Douglas Hanahan and Robert A. Weinberg (2000). The Hallmarks of Cancer. *Cell* 100: 57–70.

Douglas Hanahan and Robert A. Weinberg (2011). Hallmarks of Cancer: The Next Generation. *Cell* 144: 646-674.

[Reactome]

Antonio Fabregat, Florian Korninger, Guilherme Viteri, et. al. (2018). Reactome graph database: Efficient access to complex pathway data. *PLoS Comput. Biol.* 14(1): e1005968.

[Enrichment analysis]

F. Emmert-Streib, G.V. Glazko (2011). Pathway Analysis of Expression Data: Deciphering Functional Building Blocks of Complex Diseases. PLoS Comput. Biol. 7(5): e1002053.

[Precedents (microarrays, etc)]

Christian Pilarsky, Michael Wenzig, Thomas Specht et al (2004). Identification and Validation of Commonly Overexpressed Genes in Solid Tumors by Comparison of Microarray Data. *Neoplasia* 6: 744 – 750.

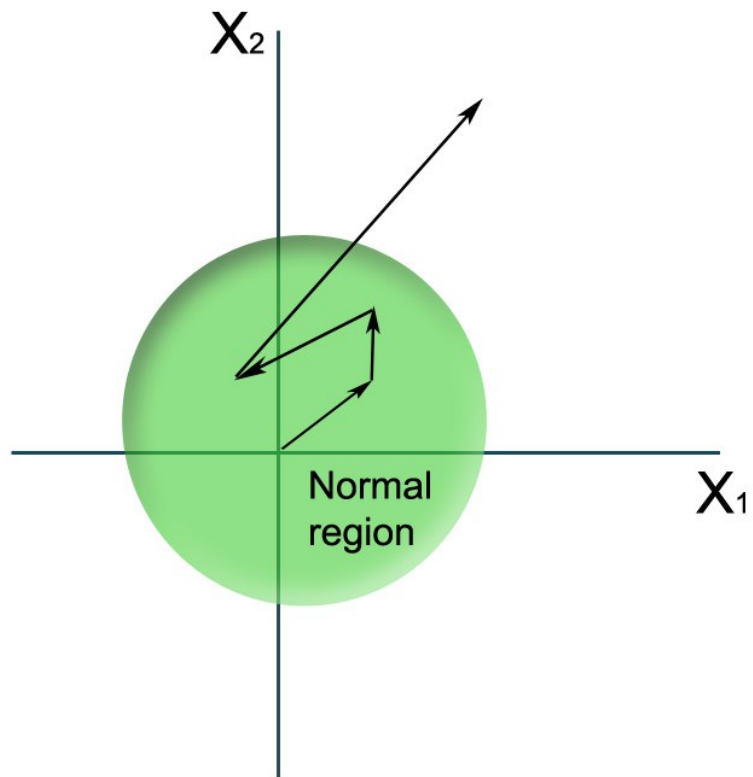


Fig. 1. Schematic representation of the somatic evolution in a tissue. The shaded area represents system oscillations within normal functioning, that is an homeostatic state composed by multiple cell niches which acts coordinately under a physiologically regulated space. Any tissue portion experiences changes, which are represented by arrows. Eventually, a niche or clone of cells may leave this area and move towards cancer.

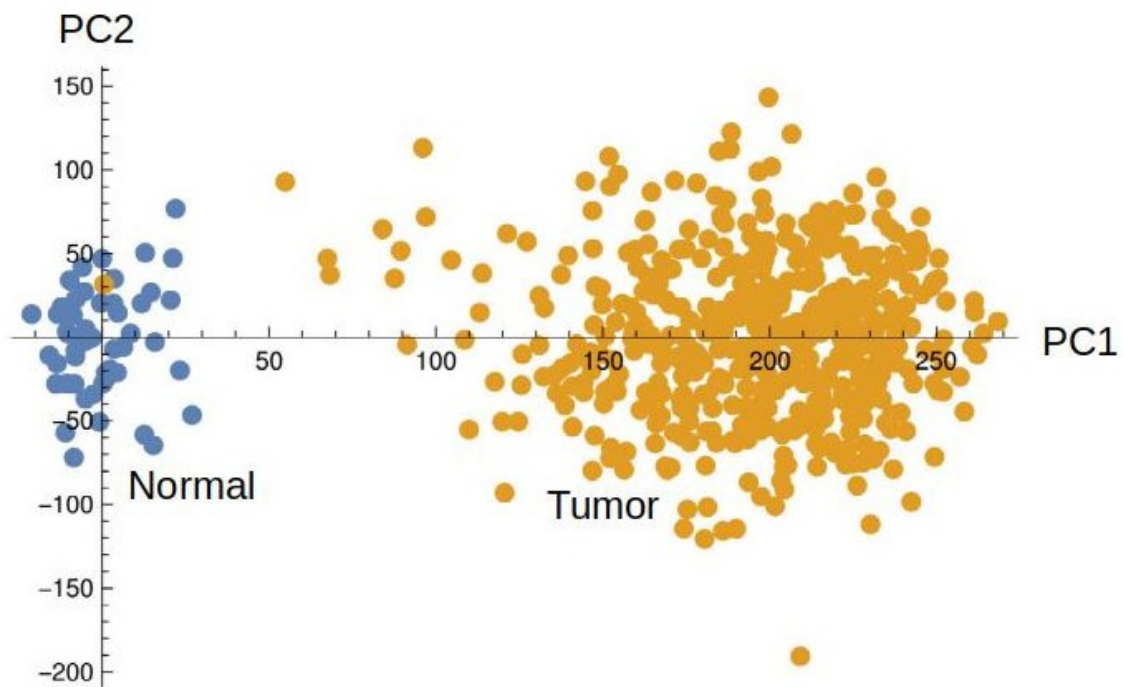


Fig. 2. Principal Component Analysis of the TCGA gene expression data for the Squamous Cell Lung Carcinoma (LUSC). This figure could be understood as a realization of the schematic view presented in Fig. 1.

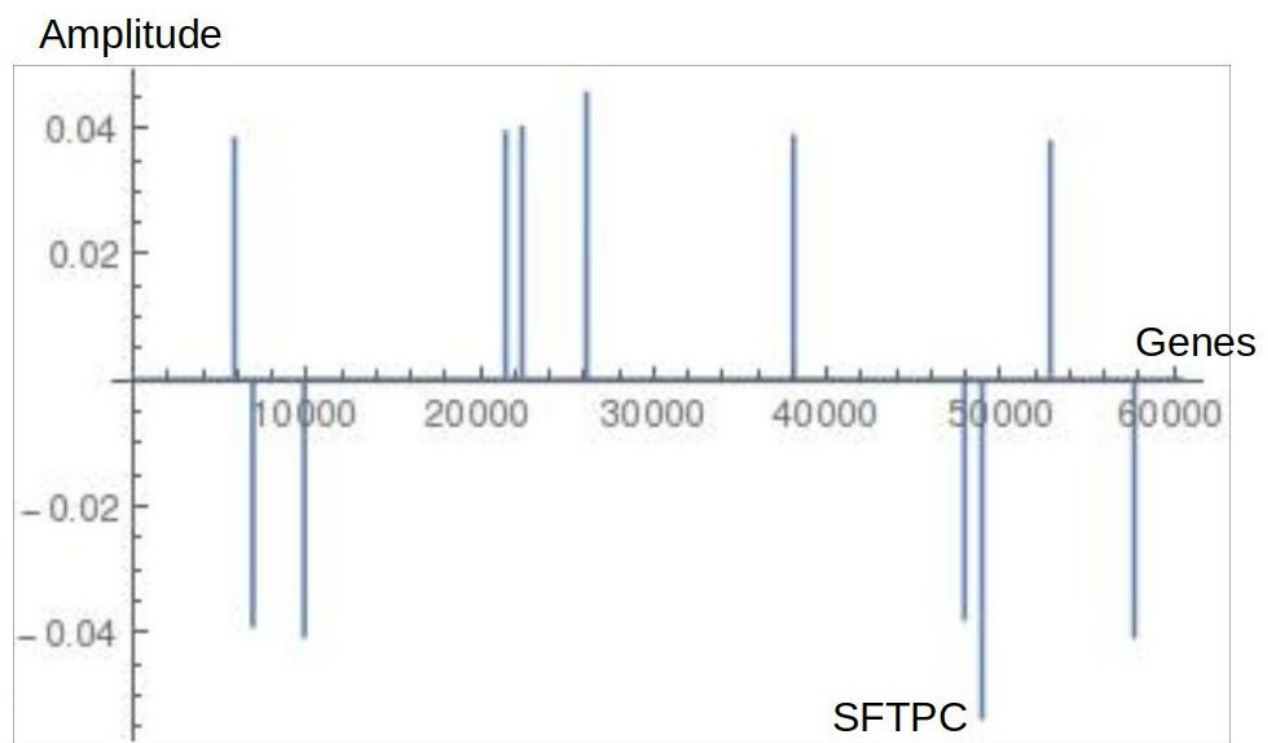


Fig. 3. Genes with the most significant contributions to the unitary vector along PC1 in LUSC. The numbering of genes is the one used in the TCGA data. To simplify drawing, the contributions of the remaining genes are set to zero. Positive signs correspond to over-expressed, and negative to sub-expressed genes. The gene with the most important contribution (Surfactant protein C, SFTPC) is indicated.

Number of
genes

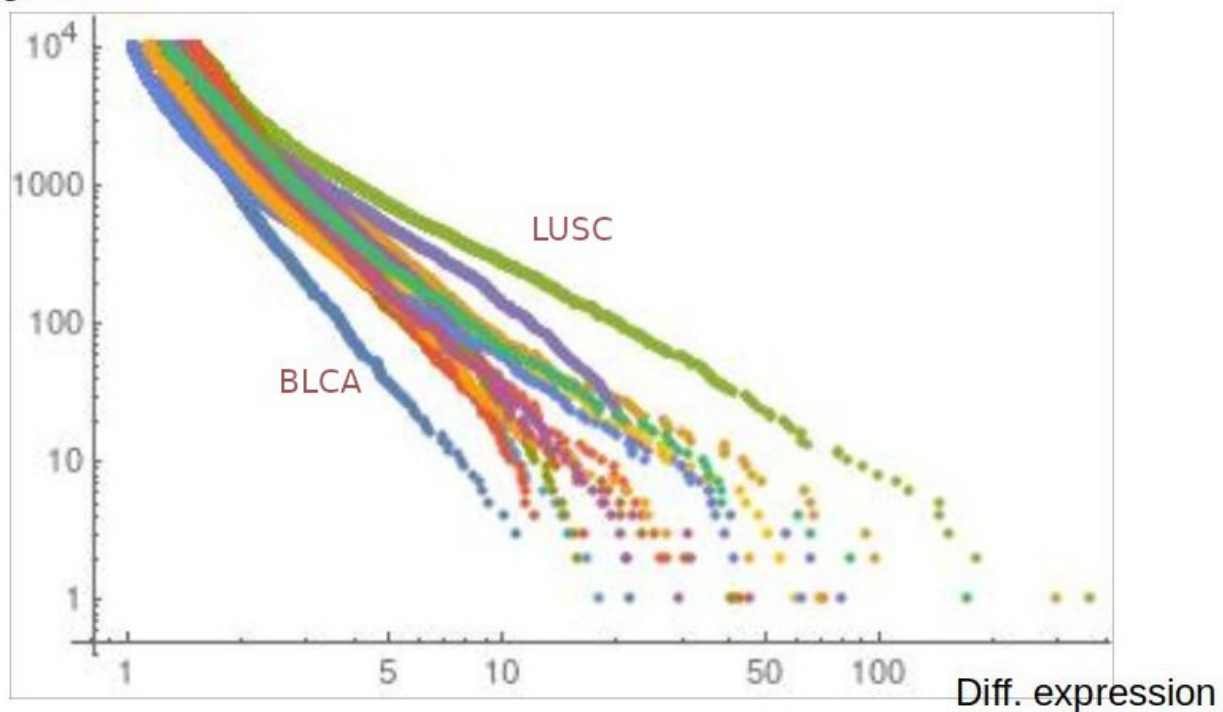


Fig. 4. The high over-expression tail in the distribution function. All of the tumors exhibit a power-like (Pareto) dependence for the number of genes with expression greater than a given value as a function of the differential expression. The extreme cases are BLCA (slope around 3 in a log-log plot) and LUSC (slope around 1.5).

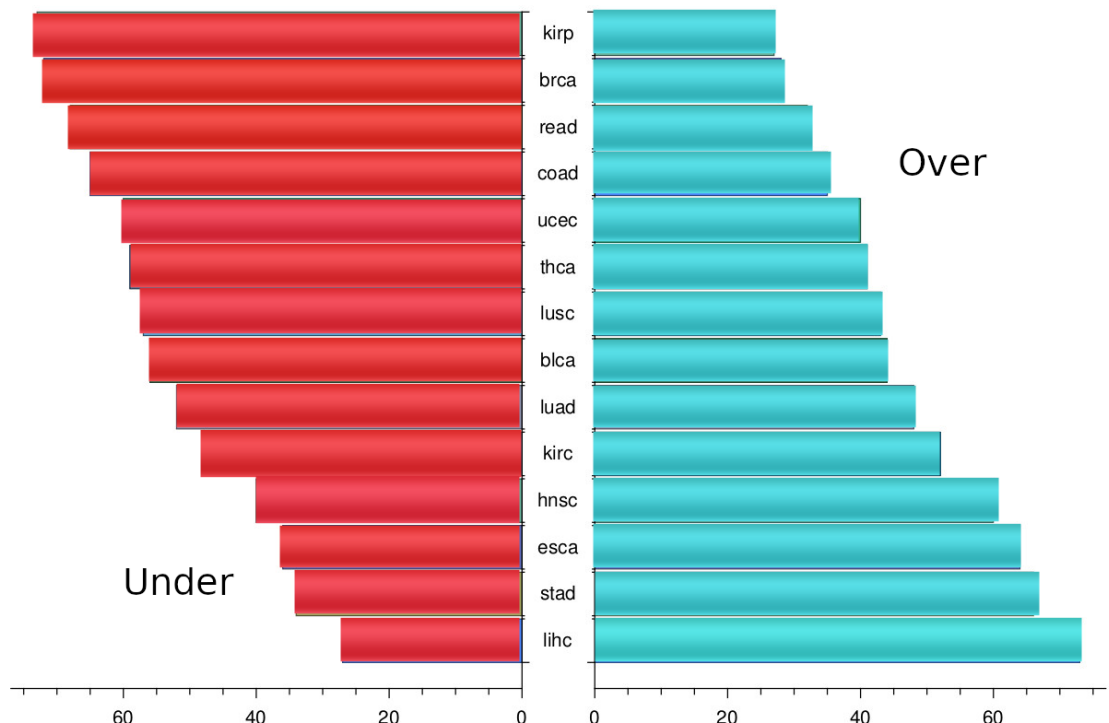


Fig. 5. Fraction (percentage) of over- and under-expressed genes in the tissues under study.
The fractions are computed in the main set of 2500 genes characterizing the tumor. Right and left scales correspond to over- and under-expression respectively.

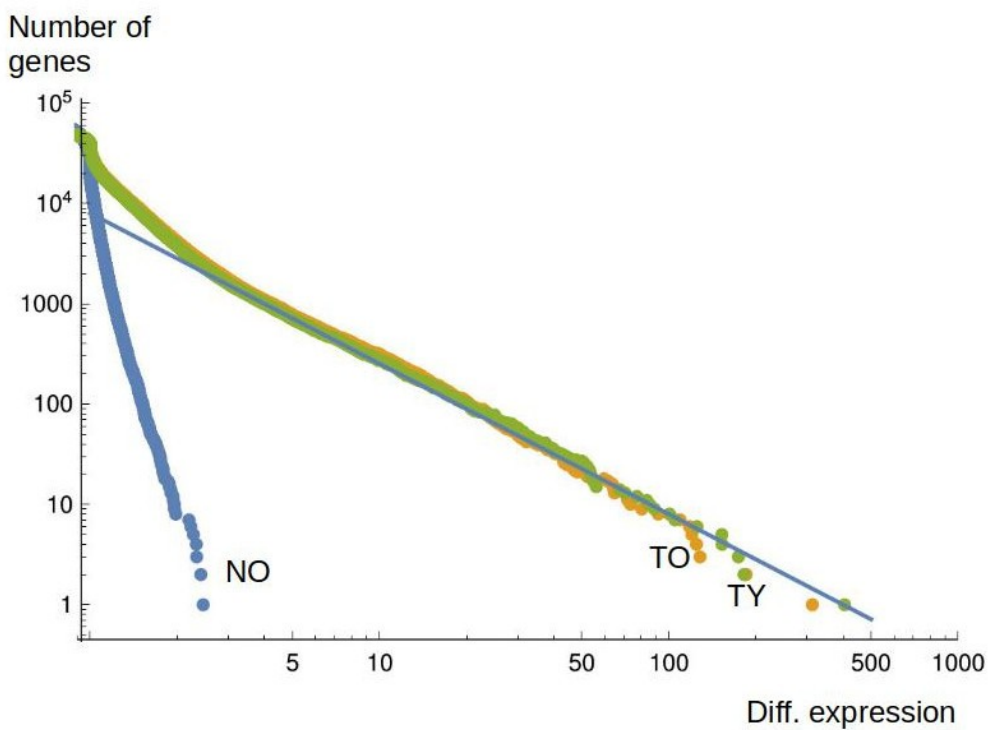


Fig. 6 Integrated gene (over) expression distribution functions in LUSC. According to age, samples are grouped into four sets: Normal Young, Normal Old, Tumor Young and Tumor Old. The average over the Normal Young set is used to define reference values to normalize the expressions. Each set of points represents the average over the respective group.

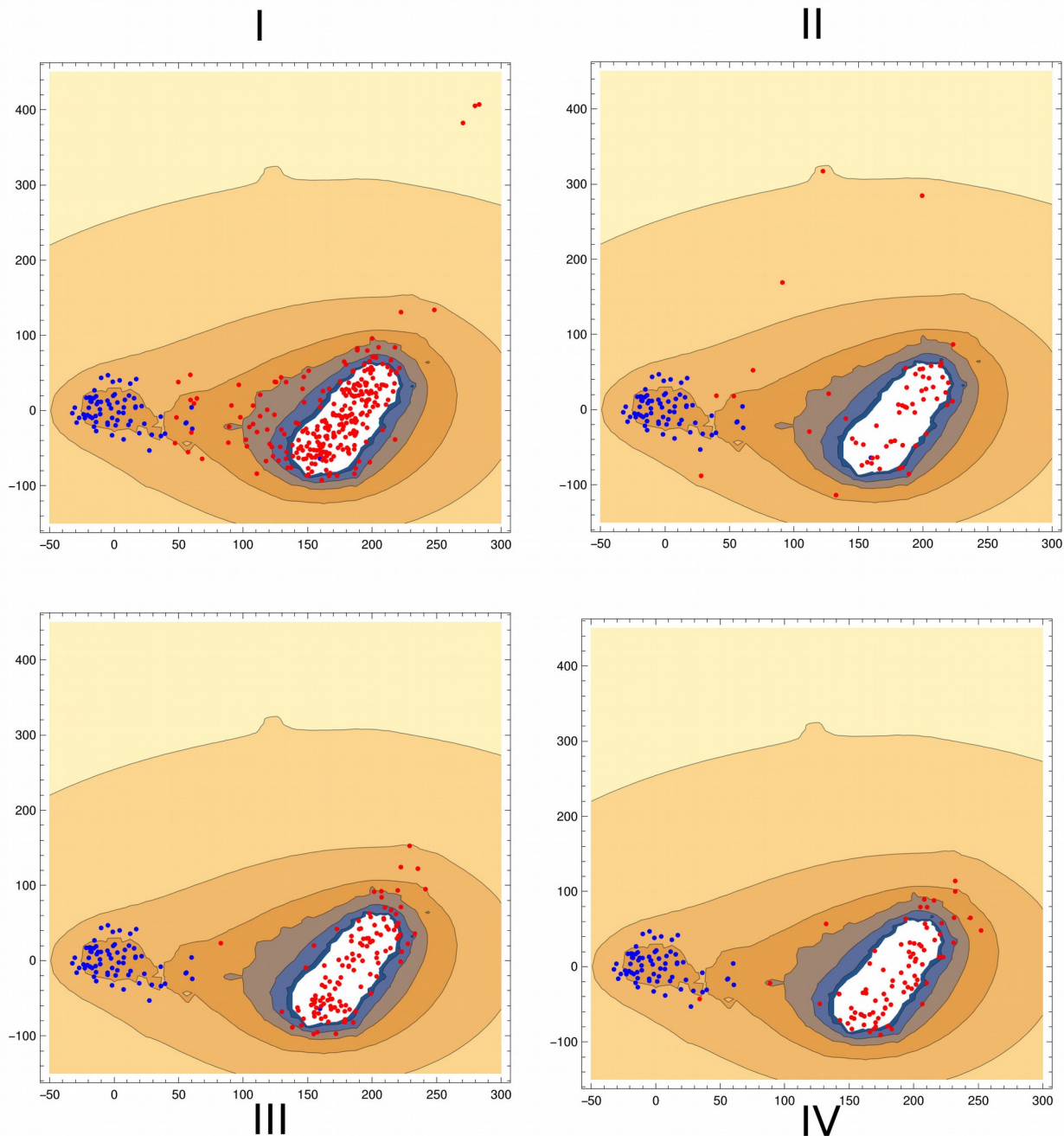


Fig. 7. Stages in the evolution of tumors in Clear Cell Kidney Cancer (KIRC). Blue points are normal tissues (included in the four panels), whereas red points are tumors in a given stage of evolution. Contours represent the total density of points. Stage i seems to be “transitional”, there are many points traveling along the intermediate region. On the other hand, stages ii, iii and iv are “final”, in the sense that most of the tumors are concentrated in the high density region. This picture reinforces the attractor paradigm of cancer. We may speculate that the attractor is the region of the state space with maximal fitness for the tumor in the given tissue.

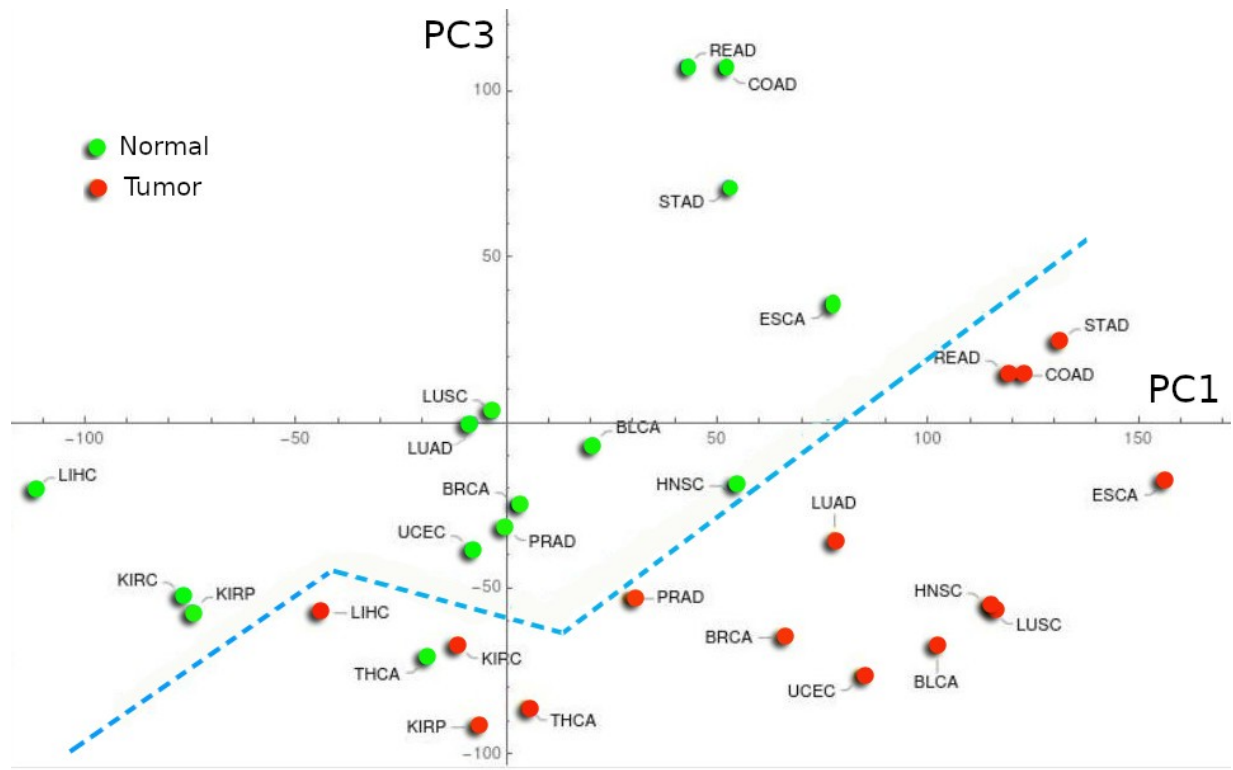


Fig. 8. The gene expression landscape in the (PC1, PC3) plane. Each point in the diagram represents the average of samples in a given localization. For simplicity, normal tissues are labeled with the corresponding tumor indexes. The approximate border between the normal and tumor regions is drawn.

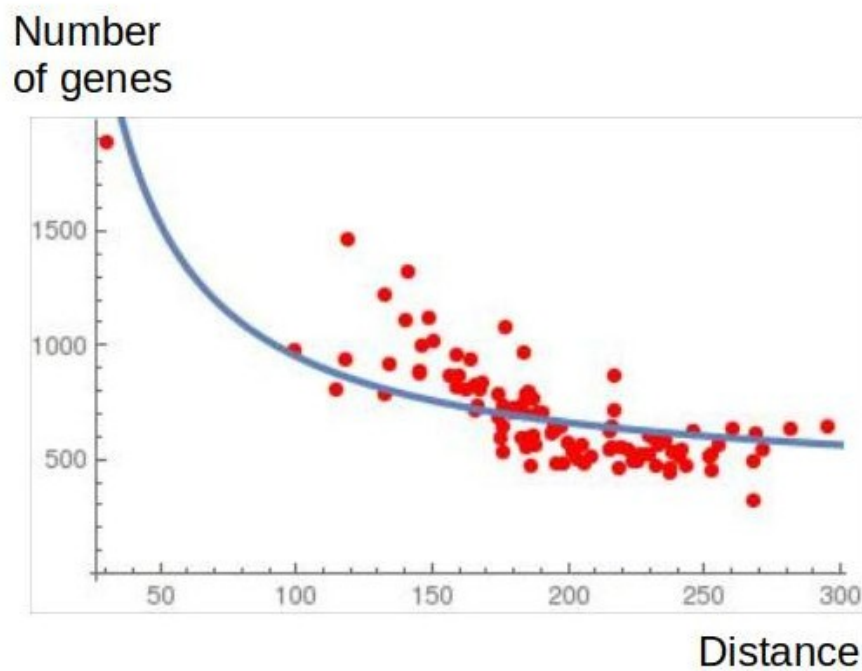


Fig. 9. The number of shared genes vs. the distances between tumor centers in pairs of tumors.
The curve is drawn only as a guide to the eye.

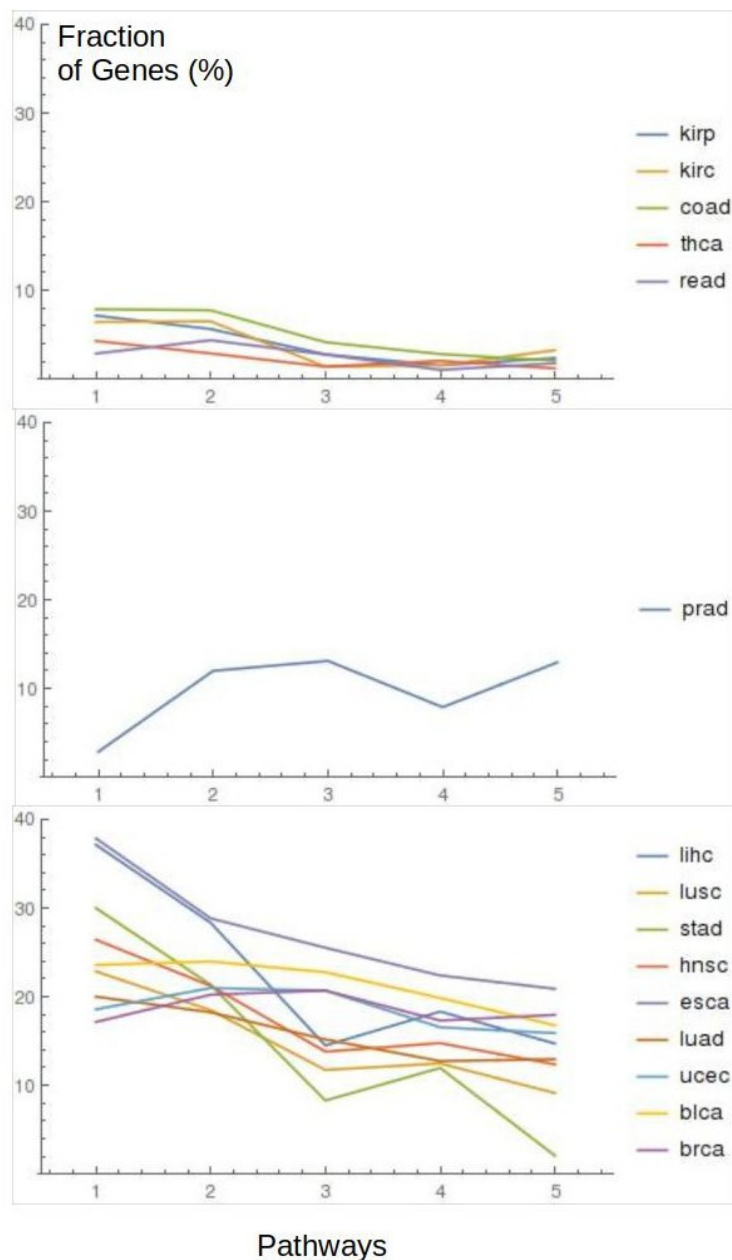


Fig. 10. Fraction of modified genes in the 5 most variable top pathways in tumors. Two groups of localizations and one independent tissue are apparent. In the x axis, pathways are numbered as follows: 1-"DNA Replication", 2-"Cell Cycle", 3-"Reproduction", 4-"DNA Repair", 5-"Chromatin organization".

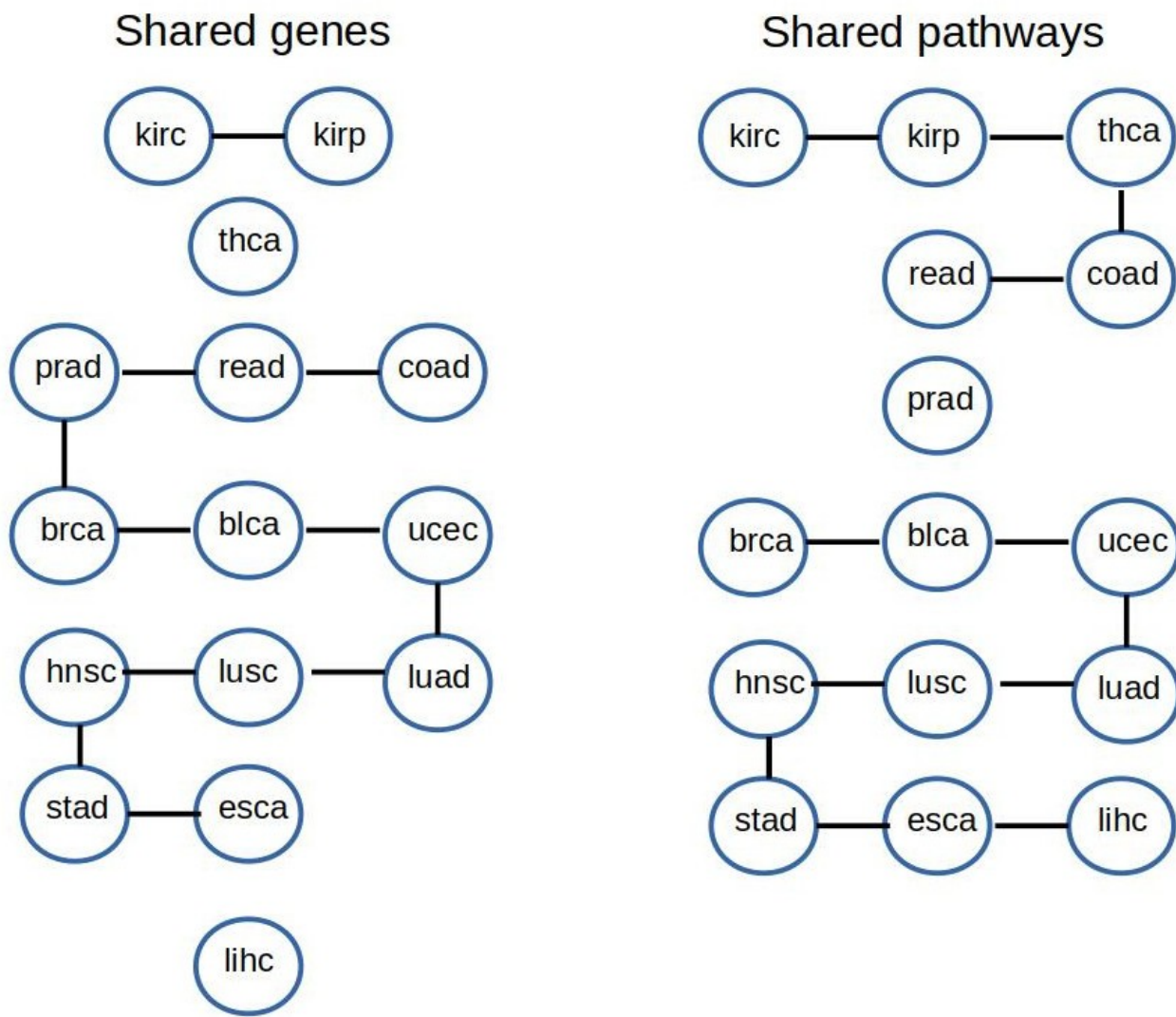


Fig. 11. Comparison between shared-genes and shared-pathways schemes for grouping tumors.

Cancer type (TCGA notation)	Normal samples	Tumor samples	Percentage of variance captured by the first 3 PCs	Maximal differential expression	Percentage of over expressed genes
KIRP	32	289	67 %	43	27 %
KIRC	72	539	72 %	300	52 %
PRAD	52	499	56 %	22	46 %
LUSC	49	502	74 %	364	43 %
LUAD	59	535	65 %	42	48 %
UCEC	23	552	65 %	80	40 %
BLCA	19	414	61 %	18	44 %
COAD	41	473	69 %	60	35 %
ESCA	11	160	55 %	30	64 %
LIHC	50	374	64 %	40	73 %
STAD	32	375	57 %	72	66 %
BRCA	112	1096	66 %	70	28 %
HNSC	44	502	60 %	45	60 %
THCA	58	510	68 %	62	41 %
READ	10	167	67 %	170	32 %

Table I. The set of data analyzed in the paper. The fraction of variance captured by the first three PCs, the maximal differential expression, and the fraction of over-expressed genes in the main 2500 genes characterizing the tumors are presented.

	KIRC	PRAD	LUSC	LUAD	UCEC	BLCA	COAD	READ	ESCA	STAD	BRCA	HNSC	LIHC	THCA
KIRP	1213	534	642	625	696	643	543	545	532	464	646	523	459	600
KIRC		488	507	551	493	472	537	516	558	455	468	576	462	475
PRAD			561	608	774	789	621	712	573	597	730	581	485	481
LUSC				1454	857	932	634	591	1011	699	871	805	539	531
LUAD					863	883	801	731	778	803	908	725	628	528
UCEC						1313	710	831	702	784	1118	691	502	583
BLCA							813	935	817	965	1101	785	615	562
COAD								1889	682	994	722	622	512	517
READ									587	951	761	567	450	518
ESCA										977	697	1069	639	502
STAD											700	859	630	433
BRCA												707	555	589
HNSC													612	485
LIHC														314

Table II. Number of common genes in the PC1 vectors for pairs of localizations.

Supplementary material

TRANSPARENT METHODS

The results of the paper are based on the analysis of TCGA data for gene expression in FPKM format. The number of genes is 60483. This is the dimension of matrices in the Principal Component analysis.

We selected the 15 cancer types shown in Table I on the basis of two conditions: i) The number of normal samples is greater than 10, and ii) There number of tumor samples is greater than 160.

We show in Fig. S1 expressions from a typical data file (PRAD case). Notice that there are around 28000 not transcribed genes (expression exactly zero), and only around 25000 genes with expression above 0.1.

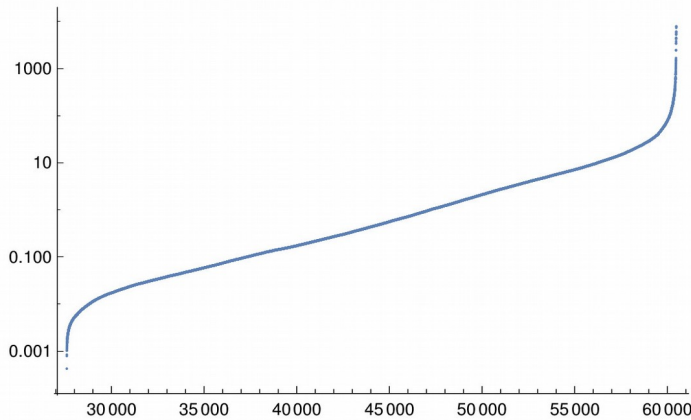


Fig. S1 (Supplementary Fig. 1). Range of values in a typical data file. Roughly half of the 60000 genes are not transcribed.

Usually, in order to compute the average expression of a gene the median or the geometric mean are used. We prefer geometric averages, but then the data should be slightly distorted to avoid zeroes. To this end, we added a constant 0.1 to the data. By applying this regularization procedure, genes identified as relevant could be under question if the differential expression is relatively low and their expression in normal tissues is near zero. As we are mainly interested in the strongly over- or under-expressed genes, they are out of the question.

For each cancer localization, we take the mean geometric average over normal samples in order to define the reference expression for each gene, e_{ref} . Then the normalized or differential expression is defined as: $\bar{e} = e/e_{ref}$. The fold variation is defined in terms of the logarithm $\hat{e} = \text{Log2}(\bar{e})$. Besides reducing the variance, the logarithm allows treating over- and sub-expression in a symmetrical way.

Deviations and variances are measured with respect to $\hat{e} = 0$. That is, with respect to the average over normal samples. This election is quite natural, because normal samples are the majority in a population, individuals with cancer are rare.

With these assumptions, the covariance matrix is written:

$$\sigma^2_{ij} = \sum \hat{e}_i(s) \hat{e}_j(s) / N_{samples}$$

where the sum runs over the samples, s , and $N_{samples}$ is the total number of samples. $\hat{e}_i(s)$ is the fold variation of gene i in sample s .

As mentioned, the dimension of matrix σ^2 is 60483. By diagonalizing it, we get the axes of maximal variance: the Principal Components (PCs). They are sorted in descending order of their contribution to the variance.

In LUSC, for example, PC1 accounts for 67% of the variance. This large number is partly due to our choice of the reference, $\hat{e} = 0$, and the fact that most of the samples are tumors. The reward is that PC1 may be defined as the cancer axis. The projection over PC1 defines whether a sample is classified as normal or tumor.

The next PCs account for a smaller fraction of the variance. PC2 is responsible of 4%, PC3 of 3%, etc. 10 PCs are enough for an approximate description of the region of the gene expression space occupied by the set of samples.

Thus, we need only a small number of the eigenvalues and eigenvectors of σ^2 . To this end, we use a Lanczos routine in Python language, and run it in a node with 2 processors, 12 cores and 64 GB of RAM memory. As a result, we get the first 100 eigenvalues and their corresponding eigenvectors.